Field Induced Quantum Confinement in Indirect Semiconductors: Quantum Mechanical and Modified Semiclassical Model

William G. Vandenberghe*† , Bart Sorée *‡, Wim Magnus *‡, Guido Groeseneken*†,
Anne S. Verhulst* and Massimo V. Fischetti§
* imec, B-3001, Leuven, Belgium
†Katholieke Universiteit Leuven, Department of Electrical Engineering, B-3001 Leuven, Belgium
‡Universiteit Antwerpen, Department of Physics, B-2020, Wilrijk, Belgium
§Department of Materials Science and Engineering, University of Texas Dallas, Richardson, Texas 75080, USA

***Abstract*—Going beyond the existing semiclassical approach to calculate band-to-band tunneling (BTBT) current we have developed a quantum mechanical model incorporating confinement effects and multiple electron and hole valleys to calculate the tunnel current in a tunnel field-effect transistor. Comparison with existing semiclassical models reveals a big shift in the onset of tunneling due to energy quantization. We show that the big shift due to quantum confinement is slightly reduced by taking penetration into the gate dielectric into account. We further propose a modified semiclassical model capable of accounting for quantum confinement.**

I. Introduction

On the one hand, nanosized MOSFETs suffer from gate-induced drain leakage (GIDL) which deteriorate their off-current [1]. On the other hand, tunnel field-effect transistors (TFETs) are considered potential candidates to overcome the limit of the 60 mV/decade subthreshold swing in a MOSFET operating at room temperature [2]. In both instances the Band-to-Band tunneling (BTBT) process is responsible for the tunneling current as illustrated in Fig. 1. An accurate theory of BTBT is therefore highly desirable.

The calculation of BTBT current is traditionally based on semiclassical models using band diagrams inside the device [3], [4]. An electron tunneling from valence to conduction band is mimicked as a classical particle disappearing at the valence band edge and reappearing at the conduction band edge, as shown in Fig. 2. Correspondingly, the tunnel current equals the integral of a tunnel generation rate G over the entire device,

$$I_{\text{semiclassical}} = q \int G \mathrm{d}V \tag{1}$$

where G can be obtained from Kane's model for direct [5] or indirect semiconductors [6]–[8].

To compare semiclassical results with quantum mechanical results, we study a TFET device with a large gate-source overlap as shown in Fig. 3. The potential can be taken to vary only in the direction perpendicular to the semiconductor-dielectric interface (z direction) [9] facilitating modeling and interpretation. In this paper, we treat tunneling in an indirect

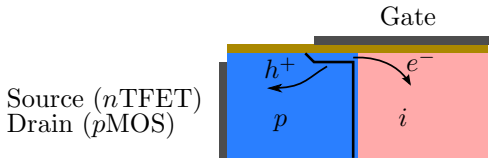

Fig. 1. Picture of GIDL/TFET working principle showing hole and electron generation due to BTBT

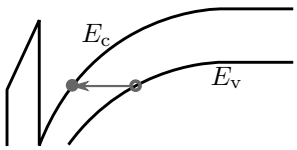

Fig. 2. Semiclassical picture of band-to-band tunneling

semiconductor and make a quantum mechanical calculation of the so-called line tunneling current component, which is proportional to the gate-source overlap. In section II, we outline the quantum mechanical framework to calculate current similar to [8] but now also including penetration into the gate dielectric. In section III, we propose a modification of existing semiclassical models to account for quantum confinement and discuss some further limitations of the semiclassical models.

II. Quantum Mechanical Modeling of BTBT

To obtain a quantum mechanical estimate of the BTBT in indirect semiconductors, we use the method outlined in [10].

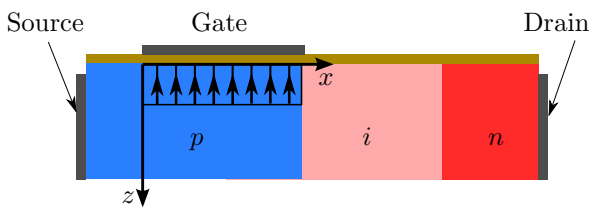

Fig. 3. Illustration of a TFET with the gate over the source, arrows indicate tunneling

978-1-61284-418-3/11/$26.00 © 2011 IEEE

First, the conduction and valence band electron wavefunctions have to be determined. Adopting the effective mass approximation for both carrier types, the Schrödinger equations read:

$$\left(E_{0\mathrm{v(c)}} \pm \frac{\hbar^2}{2}\left(\boldsymbol{\nabla}\cdot\left[m^*_{\mathrm{v(c)}\alpha}\right]^{-1}\boldsymbol{\nabla}\right) + U_{\mathrm{ext}}(z)\right)\chi_{\mathrm{v(c)}\alpha;\ell}(\mathbf{r}) = E_{\mathrm{v(c)}\alpha;\ell}\chi_{\mathrm{v(c)}\alpha;\ell}(\mathbf{r}). \quad (2)$$

We consider all six [100] oriented conduction band valleys as well as the three valence band valleys. Solving the Schrödinger equation results in a complete set of wavefunctions $\chi_{\mathrm{v(c)}\alpha;\ell}(\mathbf{r})$ and the corresponding energy eigenvalues $E_{\mathrm{v(c)}\alpha;\ell}$ where ℓ denotes the set of quantum numbers and α is the valley index.

Defining the spectral functions as

$$A_{\mathrm{v(c)}\alpha}(\mathbf{r},\mathbf{r}';E) = 2\pi\sum_{\ell}\chi_{\mathrm{v(c)}\alpha;\ell}(\mathbf{r})\,\delta(E-E_{\mathrm{v(c)}\alpha;\ell})\chi^*_{\mathrm{v(c)}\alpha;\ell}(\mathbf{r}'), \quad (3)$$

the different contributions to the charge density are determined by weighing the spectral functions with the Fermi-Dirac distribution functions $f_{\mathrm{v(c)}}(E) = 1/(1+\exp((E-\mu_{\mathrm{v(c)}})/(kT))$:

$$\rho_{\mathrm{net}}(z) = -qN_{\mathrm{a}} + 2q\int\frac{\mathrm{d}E}{2\pi}\Big((1-f_{\mathrm{v}}(E))\sum_{\alpha}A_{\mathrm{v}\alpha}(z,z;E) - f_{\mathrm{c}}(E)\sum_{\alpha}A_{\mathrm{c}\alpha}(z,z;E)\Big) \quad (4)$$

with N_{a} the doping concentration. The potential energy $U_{\mathrm{ext}}(z)$ reflecting all bias voltages can be determined by solving the 1D-Poisson equation self-consistently with the wavefunctions.

Taking the interaction with the phonons into account, we compute the phonon-assisted current from

$$I = -\frac{2e}{\hbar}\int\frac{\mathrm{d}E}{2\pi}\Big(\big(f_{\mathrm{v}}(E)(1-f_{\mathrm{c}}(E-\hbar\omega_{\mathbf{k}_0}))(\nu(\hbar\omega_{\mathbf{k}_0})+1) - f_{\mathrm{c}}(E-\hbar\omega_{\mathbf{k}_0})(1-f_{\mathrm{v}}(E))\nu(\hbar\omega_{\mathbf{k}_0})\big)T^{\mathrm{em}}_{\mathrm{v}}(E) + \big(f_{\mathrm{v}}(E)(1-f_{\mathrm{c}}(E+\hbar\omega_{\mathbf{k}_0}))\nu(\hbar\omega_{\mathbf{k}_0}) - f_{\mathrm{c}}(E+\hbar\omega_{\mathbf{k}_0})(1-f_{\mathrm{v}}(E))(\nu(\hbar\omega_{\mathbf{k}_0})+1)\big)T^{\mathrm{abs}}_{\mathrm{v}}(E)\Big) \quad (5)$$

with

$$T^{\mathrm{abs,em}}_{\mathrm{v}}(E) = \Omega\,|M'_{\mathbf{k}_0}|^2 \times\sum_{\alpha,\alpha'}\int\mathrm{d}^3r\,A_{\mathrm{v}\alpha}(\mathbf{r},\mathbf{r};E)\,A_{\mathrm{c}\alpha'}(\mathbf{r},\mathbf{r};E\pm\hbar\omega_{\mathbf{k}_0}). \quad (6)$$

At the gate dielectric ($z = 0$), a boundary condition for the wavefunctions is required. A first approximation is to use Dirichlet boundary conditions: $\chi(0) = 0$ [8]. This corresponds to modeling the gate dielectric as a hard wall potential that strictly confines the electrons to the device region.

However, real devices are found to suffer from wavefunction penetration into the dielectric. In general the penetration leads to an unwanted gate leakage current but for the field induced quantum confinement, the penetration of the gate dielectric will make the impact of confinement slightly less pronounced. To account for penetration into the dielectric, we assume the dielectric is infinitely thick and that the wavefunction decays with a given decay length l_{dec} inside the dielectric, i.e. $\chi(z) \propto \exp(z/l_{\mathrm{dec}})$ for $z < 0$. The boundary condition for the wavefunction is now:

$$\left.\frac{\mathrm{d}\chi(z)}{\mathrm{d}z}\right|_{z=0} = \frac{\chi(0)}{l_{\mathrm{dec}}}. \quad (7)$$

The value of l_{dec} can be determined from the complex band structure and is about 3 Å for HfO_2 [11].

In Fig. 4, the quantum mechanical current is compared with the semiclassical current for two different doping concentrations. The big onset shift between the semiclassical and the quantum mechanical calculation is due to the quantum confinement of the electrons near the interface. The shift is bigger for the device with the larger doping concentration as larger fields and stronger carrier confinement is present. The two different effective masses (transversal and longitudinal) in the z direction give rise to different energy levels, the signatures of which can be clearly observed as a cusp in the current-voltage characteristic for the TFET with high doping concentration. The shift due to confinement can be seen to be smaller when the penetration into the gate dielectric is taken into account.

III. Semiclassical models

In this section we propose a modification to the semiclassical model to account for quantum confinement.

A. The existing semiclassical model

The semiclassical model we have used for our comparison in Fig. 4 is similar to that used in Ref. [10] and defines two tunnel paths starting at the valence band and ending at the conduction band: one corresponding to a path bridging a gap $E_{\mathrm{g}} + \hbar\omega_{\mathbf{k}_0}$ and the other bridging a gap $E_{\mathrm{g}} - \hbar\omega_{\mathbf{k}_0}$. The first path corresponds either to an electron going from valence to conduction band emitting a phonon or an electron going in the other direction absorbing a phonon. The second path describes the dual processes.

Based on the tunnel path start point ($z = z_1$) and end point ($z = z_2$), illustrated in Fig. 5, the path length ($l_{\mathrm{tun}} = z_2 - z_1$) is determined and a generation rate is calculated according to the average force $\bar{F} = (U_{\mathrm{ext}}(z_2) - U_{\mathrm{ext}}(z_1))/l_{\mathrm{tun}}$ along the tunnel path. To have a fair comparison between the quantum mechanical and the semiclassical model we have taken the same parameters for the electron-phonon interaction strength, effective masses and bandgap and substituted them in the indirect Kane model [7], [10]. Only the tunneling of the light holes to the electrons with their transversal mass in the tunneling direction has been taken into account as this process dominates over the other tunneling processes.

B. Modified semiclassical model

As observed in Fig. 4, the major discrepancy between the semiclassical and the quantum mechanical input characteristics is the big shift in onset voltage due to the absence of states to tunnel into due to quantum confinement. Based on this

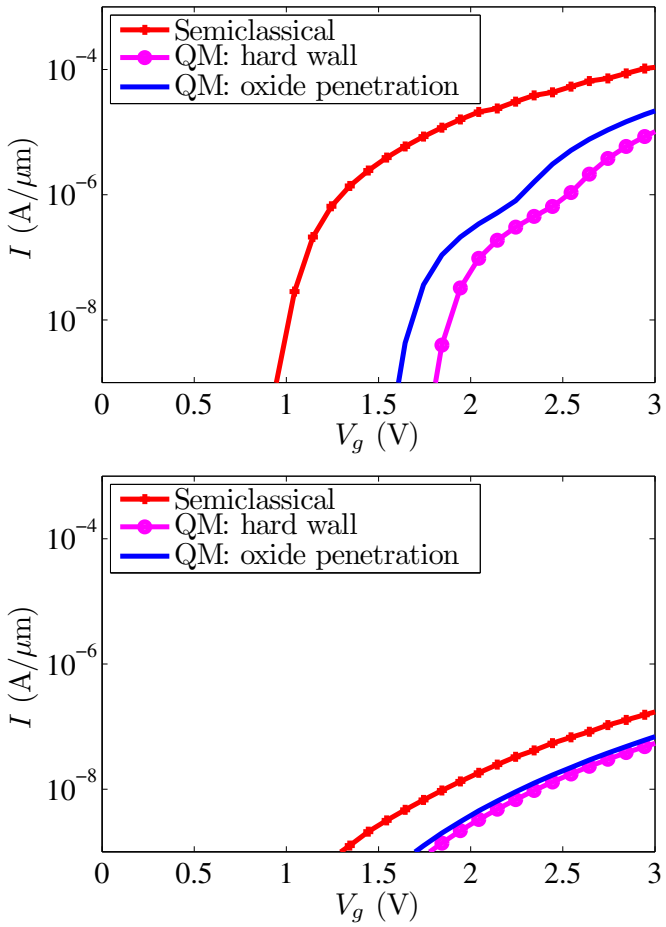

Fig. 4. Comparison of full quantum mechanical current with semiclassical current for source doping $N_\mathrm{a} = 10^{20}$ cm^{-3} (top) and $N_\mathrm{a} = 10^{19}$ cm^{-3} (bottom) revealing the big shift due to quantum confinement for the hard wall condition and taking penetration into the gate dielectric into account. Lower doping results in a reduced effect of quantum confinement. Additional parameters used for the calculation are given in the Appendix.

observation we propose a modified semiclassical model which proceeds as follows: 1) start a tunnel path at an initial position z_1 in the valence band, 2) determine the location of the intersection of the tunnel path with the conduction band z_2, 3) determine the depth of the conduction band well at the intersection with the dielectric interface ΔE_c, 4) determine a minimum well depth $\Delta E_\mathrm{min,c}$ required to accomodate a particle, 5) if $\Delta E_\mathrm{c} > \Delta E_\mathrm{min,c}$ calculate generation rate in normal fashion, otherwise reject the tunnel path. An illustration of an accepted and a rejected path is given in Fig. 5.

To estimate the minimal well depth required to accomodate a particle, calculate the energy level of the first state in the triangular well approximation

$$E_\mathrm{0c} = -a_0 \left(\frac{\hbar^2 \left(F(z_2)\right)^2}{2m^*_{\mathrm{c},z}} \right)^{1/3} \tag{8}$$

with $a_0 \approx -2.3381$ the first zero of the Airy function, $m^*_{\mathrm{c},z}$

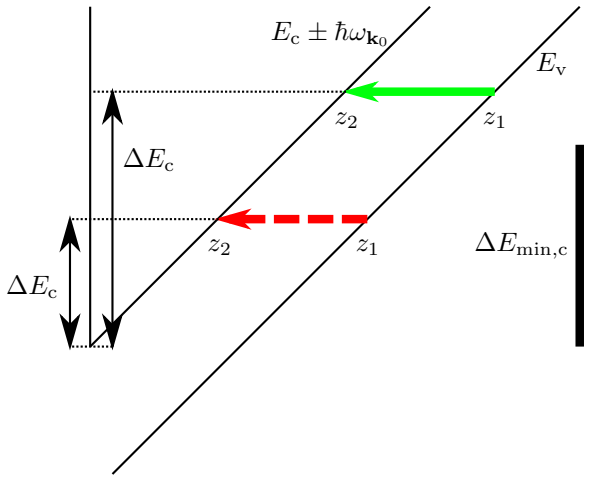

Fig. 5. Illustration of how a semiclassical path starting at z_1 going to z_2 is defined. For the modified semiclassical model the well depth ΔE_c at the interface has to be determined. Tunneling either proceeds in the normal fashion if $\Delta E_\mathrm{c} > \Delta E_\mathrm{min,c}$ (solid path) or the tunnel path is rejected $\Delta E_\mathrm{c} \leq \Delta E_\mathrm{min,c}$ (dashed path).

is the effective mass in the z-direction and where

$$F(x_2) = -\frac{\mathrm{d}}{\mathrm{d}z} U_\mathrm{ext}(z)\Big|_{z=z_2} \tag{9}$$

is the force on the electron at $z = z_2$. In the modified semiclassical picture, the penetration into the gate dielectric can be taken into account by reducing E_0c by the energy the electron is expected to gain over the distance of the decay length:

$$\Delta E_\mathrm{min,c} = E_\mathrm{0c} - F(x_2) l_\mathrm{dec}. \tag{10}$$

We have implemented the modified semiclassical model outlined above and compared it with the previously calculated current-voltage characteristics and show the result in Fig. 6. One more change that was made in the modified semiclassical model shown in Fig. 6 is that tunneling of both the transversal and the longitudinal electrons was taken into account. The tunneling probability is much lower for the longitudinal electrons but due to reduced impact of quantum confinement, their contribution is now also important. The modified semiclassical model manages to capture the effect of the quantum confinement and gives reasonably good agreement with the quantum mechanical result.

In our case we have studied a nTFET where the conduction band electrons are confined. In case confinement is present for the valence band electrons, it must be verified if the well for the valence band electrons is deep enough.

C. Further limitations to the semiclassical model

We have shown that semiclassical models can be adapted to incorporate field induced quantum confinement. Nevertheless, we believe it is important to remind the reader that there are still some other unsolved issues with the use of semiclassical models we have not discussed in this paper.

First of all, in a two-dimensional potential profile, tunnel paths are chosen in the device according to straight lines [12],

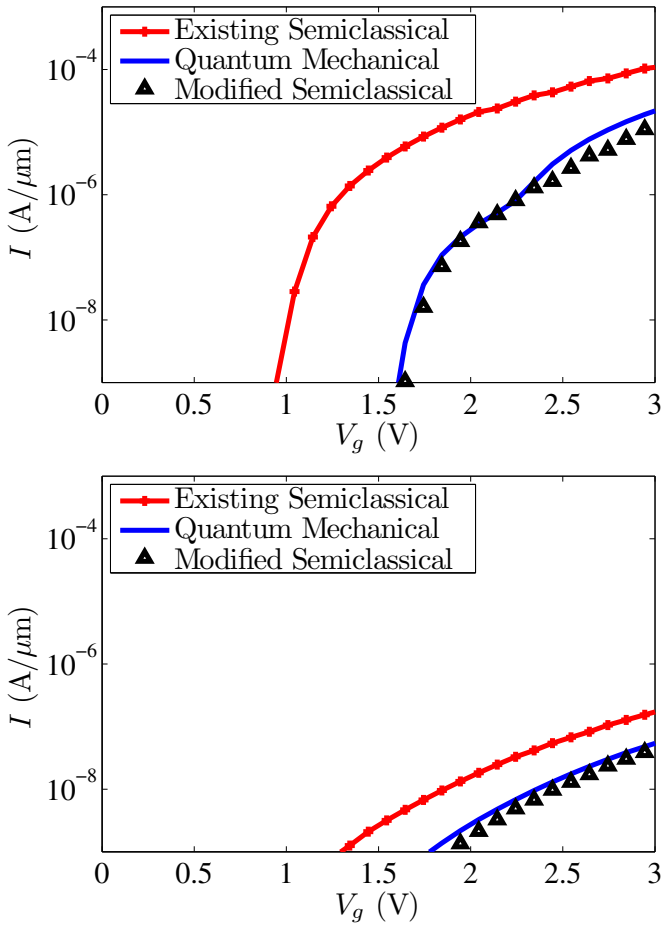

Fig. 6. Full quantum mechanical current and the existing semiclassical current for source doping $N_\mathrm{a} = 10^{20}$ at/cm^{-3} (top) and $N_\mathrm{a} = 10^{20}$ at/cm^{-3} (bottom) as given in Fig. 4 compared with the modified semiclassical model. Wavefunction penetration is taken into account.

along the electric field lines [13] or along Newtonian trajectories [14]. For a potential with pronounced two-dimensional features, none of these methods can be justified on theoretical grounds and certainly not for the case of phonon-assisted tunneling where the interaction with the phonon has to be accounted for.

Secondly, the electron/hole generation is assumed to take place at the edge of the conduction and valence band when introduced in the drift-diffusion equations. Again no theoretical framework on how the generation should be incorporated is available.

IV. Conclusion

In a semiconductor device with high electric fields near the gate-dielectric, taking quantum confinement effects into account when calculating BTBT is paramount and existing semiclassical models fail. Penetration of the wavefunction into the gate dielectric slightly reduces the quantum confinement effect compared to semiclassical results. We have also demonstrated a modified semiclassical model which amounts to a small correction of the existing models and which is capable of capturing the effect of field-induced quantum confinement.

Acknowledgments

William Vandenberghe gratefully acknowledges the support of a Ph.D. stipend from the Institute for the Promotion of Innovation through Science and Technology in Flanders (IWT-Vlaanderen). This work was supported by imec's Industrial Affiliation Program.

Appendix

Parameters used:
Bandgap: 1.12 eV
Effective masses: $m_{\mathrm{c,l}}$ = 0.9163 m_0, $m_{\mathrm{c,t}}$ = 0.1905 m_0, $m_{\mathrm{v,lh}}$ = 0.16 m_0 and $m_{\mathrm{v,hh}}$ = 0.490 m_0
Dielectric constants: $\epsilon_\mathrm{s} = 11.5\epsilon_0$ and $\epsilon_\mathrm{ox} = 15\epsilon_0$
Oxide thickness and gate length: $t_\mathrm{ox} = 2$ nm and $L = 30$ nm
Electron-phonon parameters: $\hbar\omega_{\mathbf{k}_0} = 18.4$ meV, $\Omega|M'_{\mathbf{k}_0}|^2 = 4.8634 \times 10^{-31}$ eV^2 m^3

References

[1] T. Chan, J. Chen, P. Ko, and C. Hu, "The impact of gate-induced drain leakage current on MOSFET scaling," *Electron Devices Meeting, 1987 International*, vol. 33, pp. 718–721, 1987.
[2] S. Banerjee, W. Richardson, J. Coleman, and A. Chatterjee, "A new three-terminal tunnel device," *Electron Device Letters, IEEE*, vol. 8, no. 8, pp. 347 – 349, Aug. 1987.
[3] K. K. Bhuwalka, J. Schulze, and I. Eisele, "A simulation approach to optimize the electrical parameters of a vertical tunnel FET," *IEEE Transactions on Electron Devices*, vol. 52, no. 7, July 2005.
[4] A. S. Verhulst, W. G. Vandenberghe, K. Maex, and G. Groeseneken, "A tunnel field-effect transistor without gate-drain overlap," *Applied Physics Letters*, vol. 91, no. 053102, July 2007.
[5] E. O. Kane, "Zener tunneling in semiconductors," *Journal of Physics and Chemistry of Solids*, vol. 12, pp. 181–188, 1959.
[6] L. Keldysh, "Influence of the lattice vibrations of a crystal on the production of electron-hole pairs in a strong electric field," *Sov. Phys. JETP*, vol. 7, p. 665, 1959.
[7] E. O. Kane, "Theory of tunneling," *Journal of Applied Physics*, vol. 32, no. 1, pp. 83–91, 1961.
[8] W. Vandenberghe, B. Sorée, W. Magnus, and M. V. Fischetti, "Generalized phonon-assisted zener tunneling in indirect semiconductors with non-uniform electric fields: A rigorous approach," *Journal of Applied Physics*, vol. 109, no. 12, p. 124503, 2011. [Online]. Available: http://link.aip.org/link/?JAP/109/124503/1
[9] W. G. Vandenberghe, A. S. Verhulst, G. Groeseneken, B. Sorée, and W. Magnus, "Analytical model for a tunnel field-effect transistor," in *IEEE Melecon*, 2008.
[10] W. G. Vandenberghe, B. Sorée, W. Magnus, G. Groeseneken, and M. V. Fischetti, "Impact of field-induced quantum confinement in tunneling field-effect devices," *Applied Physics Letters*, vol. 98, no. 14, p. 143503, 2011. [Online]. Available: http://link.aip.org/link/?APL/98/143503/1
[11] F. Sacconi, J. Jancu, M. Povolotskyi, and A. Di Carlo, "Full-band tunneling in high-κ oxide mos structures," *Electron Devices, IEEE Transactions on*, vol. 54, no. 12, pp. 3168 –3176, dec. 2007.
[12] *Sentaurus Device*, Synopsys, March 2010.
[13] W. G. Vandenberghe, A. S. Verhulst, G. Groeseneken, B. Sorée, and W. Magnus, "Analytical model for point and line in a tunnel field-effect transistor," in *Simulation of Semiconductor Processes and Devices, 2008 International Conference on*, Sept. 2008.
[14] C. Shen, L.-T. Yang, G. Samudra, and Y.-C. Yeo, "A new robust non-local algorithm for band-to-band tunneling simulation and its application to tunnel-fet," *Solid-State Electronics*, vol. 57, no. 1, pp. 23 – 30, 2011. [Online]. Available: http://www.sciencedirect.com/science/article/pii/S0038110110003539